

Hydraulic and Strength Performance of Missouri's Type-5 Base Material

by Jorge R. Parra and Awilda Blanco

Jorge R. Parra, PE
University of Missouri - Columbia
Doctoral Candidate
Department of Civil and Environmental Engineering
E2509 Engineering Building East
Columbia, MO 65211
Telephone: (573) 884-3862
Fax: (573) 882-4784
E-mail: jrpb66@mizzou.edu

Awilda Blanco, EIT
University of Missouri - Columbia
Graduate Candidate
Department of Civil and Environmental Engineering
E2509 Engineering Building East
Columbia, MO 65211
Telephone: (573) 884-3322
Fax: (573) 882-4784
E-mail: ab9de@mizzou.edu

Word Count: 3794 words plus (9 figures *250) plus (3 tables * 250) = 6794 words

Submitted October 18, 2002 for consideration for presentation at the 2002 Midwest Transportation Consortium Fall Student Conference

ABSTRACT

Across the state of Missouri, it has been noted that paved roads deteriorate at an accelerated rate. The base material has been identified as a possible source of the problem. To investigate this issue, researchers at the University of Missouri-Columbia have conducted in-situ and laboratory hydraulic conductivity testing, as well as cyclic triaxial testing in order to evaluate a relationship between drainage conditions and cyclic behavior of the base material. Laboratory and in-situ hydraulic conductivity testing was performed on aggregates used as base materials for medium and heavy traffic roads. A granular material from one Missouri quarry exhibiting typical engineering properties for road base application was selected for strength evaluation. Test results indicate that the hydraulic conductivity of the base material selected does not comply with requirements to assure long-term effective drainage. The shear strength properties of the compacted base material were tested following strain-controlled and stress-controlled criteria, and for saturated-undrained conditions, which represent a worst drainage scenario that a poorly performing pavement structure might experience. Results show that while the shear strength response to cyclic loads in stress-controlled conditions remains unchanged due to significant negative pore pressure build-up, rapid degradation in strength occurs in strain-controlled conditions when generation of positive pore pressures reduces effective stresses to zero during a small range of strains. Under cyclic loading conditions, the saturated base loses most of its strength within a few load cycles. This behavior could explain the premature deterioration of some pavements.

INTRODUCTION

Although the importance of well-drained pavement systems has been extensively documented, (1,2,3), the design and construction of pavement systems has not emphasized drainage for the last few decades. During this time, designers have focused on the strength of pavements, while little importance has been given to drainage of the pavement systems.

Water can flow into the base of the pavement through joints, cracks, and from groundwater sources (3). The presence of water and the lack of drainable layers in the pavement cause what can be described as a bathtub effect, owing to the fact that the pavement base remain saturated for long periods of time. The combination of saturated conditions in the road base and the cyclic loading of the pavement system due to moving vehicles cause a loss in strength and eventually pavement failure (4).

In Missouri, two principal base course systems are used beneath the pavement, as shown in Figure 1. The first is a 10-cm (4-in) layer of a well-graded aggregate with particle sizes from 25-mm (1-in) to less than 0.074-mm (0.003-in) (No. 200 sieve), referred to as Type 5 base. The alternative material consists of a 0.6-m (2-ft) layer of rock fill, and the pavement is placed directly on any of these two materials. The main objective of this project was to assess the drainability of the well-graded aggregate by performing a program of in-situ hydraulic conductivity tests and laboratory tests, and to evaluate the strength of the Type 5 base material by a series of strain-controlled and stress-controlled cyclic triaxial tests under saturated-undrained conditions. Saturated-undrained conditions can be expected in pavement layers with insufficient drainage characteristics.

MATERIALS AND METHODS

Bulk samples of the Type 5 base material were obtained from supplier quarries, on-site stockpiles, and from compacted, in-place roadway bases around Missouri. Based on Missouri Department of Transportation (MoDOT) specifications, the base material can have up to fifteen percent by weight passing the No. 200 sieve (5). Dry and wet sieve analyses were performed on all Type 5 base materials and rock fill alternates to determine the amount of fines in each material (Table 1). The last two materials listed in this table are specimens of the rock fill alternate. Individual particles in this material can be as large as 0.3-m (1-ft) and the interstices may be filled with a mixture of coarse aggregates to fines. Specimens used for the cyclic triaxial tests were prepared using the material from Lanagan Quarry because it is the material with one of the lower fines content and it is therefore expected to be the most freely draining material.

Laboratory and Field Hydraulic Conductivity Testing

The laboratory hydraulic conductivity for each material was measured using a constant head permeameter (CHP), as shown in Figure 2. The 15-cm (6-in) diameter specimens were prepared by compacting the material using standard Proctor energy, based on method C from ASTM D698 (6). Specimens were compacted to the respective maximum dry density and optimum water content for each material. MoDOT provided compaction curves for the different Type 5 base materials. The compacted specimens were placed in the permeameter, which provided flow

under a constant head, and flows per unit area under different hydraulic gradients were determined. The hydraulic conductivity was then determined by fitting a best-fit straight line to the flow per unit area vs. hydraulic gradient plot. In several cases, no flow was measured using the CHP. In general, all laboratory compacted specimens were tested in the CHP; however, the sensitivity of the device is about 1×10^{-4} -cm/sec (0.3-ft/day) below which, accurate hydraulic conductivity measurements are difficult to discern. Therefore, specimens that exhibited hydraulic conductivities lower than approximately 1×10^{-4} -cm/sec (0.3 ft/day) were removed from the CHP, set up in a flexible wall permeameter and tested according to ASTM D5084 procedures (7).

In-situ measurements of hydraulic conductivities were performed using a double ring infiltrometer (DRI) device (Figure 3). The double ring infiltrometer provides a direct determination of the infiltration rate in the material being tested (8). Infiltration rate is defined as volume per time per unit area perpendicular to flow direction, or

$$I = \frac{Q/t}{A} \quad (1)$$

where I is the infiltration rate [L]/[T], Q is the volume of infiltrated fluid [L³], t is the time of infiltration [T], and A is the area [L²] over which the liquid infiltrated.

The hydraulic conductivity can be determined by dividing the infiltration rate by the hydraulic gradient. For the cases in this study, an assumption of full-depth (10-cm or 4-in) saturation of the base was made and the hydraulic gradient was taken as:

$$i = (h+d)/d \quad (2)$$

where h is the height of water ponded above the base [L], and d is the thickness of the base [L] (Figure 3). The hydraulic conductivity is then calculated as

$$k = \frac{I}{i} \quad (3)$$

where k is the hydraulic conductivity [L]/[T], I is the measured infiltration rate and i is the hydraulic gradient.

Hydraulic conductivity values obtained from in-situ and laboratory testing were also compared with the values calculated using empirical equations. Three different methods were used to empirically estimate the hydraulic conductivity of the materials tested. All of the methods rely on the grain size distribution of the aggregate. The methods included:

A. Hazen Equation (11): $k = D_{10}^2$ (4)

where D_{10} represents the size in mm at which 10 percent of the sample by weight is smaller, and the hydraulic conductivity has units of cm/sec,

B. Sherard Equation (12): $k = 0.35D_{15}^2$ (5)

where D_{15} represents the size in mm at which 15 percent of the sample by weight is smaller, and the hydraulic conductivity has units of cm/sec,

C. Moulton Equation (3): $k = \frac{6.214 \times 10^5 D_{10}^{1.478} n^{6.654}}{P_{200}^{0.597}}$ (6)

where n represents the porosity of the material and P_{200} represents the fraction of material finer than the No. 200 sieve (0.075-mm) in percent.

Shear Strength Testing

The effective stress shear strength properties of the base materials were determined by conducting Consolidated-Undrained type triaxial tests with pore pressure measurement (\overline{CU}). This test requires 100 percent saturation of the sample prior to the consolidation and shearing stages. Although base materials are not designed to experience saturation conditions, the intention of the tests was to mimic a worst case scenario consisting of a poorly-draining material that will eventually reach this condition. Aggregate samples were compacted at their optimum water content at standard Proctor energy to form specimens of 7.4-cm (2.9-in) in diameter and 14.2-cm (5.6-in) in height. The maximum particle size used for triaxial testing was limited by the size of the compaction mold to an overall diameter of 1.27-cm (0.5-in). This maximum particle size avoids bridging problems of larger particles in the compaction mold. \overline{CU} Tests were performed at strain rates of 1.5 percent per hour, under effective confining stresses of 14, 28, and 42-kPa (2.4, and 6-psi), which are representative of the stress levels close to the ground surface. Samples were sheared to a maximum strain of 30 percent.

Cyclic Triaxial Tests

Sample dimensions, gradation, test preparation, and saturation process followed the same procedures as for the \overline{CU} type triaxial tests. The strain rate was set to 1000 percent per hour to mimic the cyclic effect produced by traffic loads as closely as possible.

Stress-controlled tests were set to stop when reaching either of the following criteria: a maximum strain of 20 percent or one hundred loading cycles. Samples at an effective stress of 14- kPa were sheared to stresses corresponding to 20 percent, 40 percent, and 60 percent of the maximum principal stress difference as determined from static \overline{CU} tests, respectively; and reloaded at about 5 percent to 10 percent of the maximum principal stress difference.

Strain-controlled tests consolidated under effective confining stresses of 14-kPa and 28-kPa, respectively, were set to shear to 100 load cycles at low strains in the range of 1 percent to 4 percent, that are representative of field conditions. A strain rate of 1000 percent per hour was again used.

RESULTS AND DISCUSSION

Hydraulic Conductivity Testing

Measured values of hydraulic conductivity from the laboratory and field tests, and estimates from empirical equations are presented in Table 2. The estimated values are primarily based on the grain size of the finer fraction as noted in the previous section. The Hazen and Sherard methods result in predictions of hydraulic conductivity ranging from 1×10^{-1} -cm/sec to 1×10^{-2} -

cm/sec (300 to 30-ft/day). Estimates of hydraulic conductivities using Moulton's expression resulted in values from 1×10^{-3} -cm/sec to 1×10^{-4} -cm/sec (3 to 0.3-ft/day).

Laboratory-measured hydraulic conductivities ranged from 1×10^{-1} -cm/sec to 1×10^{-7} -cm/sec (300 to 3×10^{-4} -ft/day) (Table 2). The laboratory and field measured values are plotted for each material in Figure 4. With some exceptions, the in-situ hydraulic conductivities are 1 to 2 orders of magnitude lower than the laboratory-measured values. In general, the in-situ hydraulic conductivities ranged from 1×10^{-4} -cm/sec to 1×10^{-5} -cm/sec (0.3 to 0.03-ft/day). Several observations regarding the difference between the laboratory and field values are justified and presented as follows. First, although the laboratory specimens were compacted near optimum water content and maximum dry density, it is likely that the final conditions of the laboratory specimens did not truly represent those of the field-compacted specimens. Laboratory compaction was performed using an impact compactor (6); however, field compaction was performed with self-propelled vibrating equipment. Second, during permeability testing in the CHP, piping of some fine particles, occasionally large amounts, was observed. While such piping will increase the hydraulic conductivity of the laboratory specimens, no such piping was observed in the field tests. Given these two observations, it is understandable that the field hydraulic conductivity would tend to be lower than the laboratory-measured hydraulic conductivity.

The field and laboratory-measured hydraulic conductivities are plotted versus the predicted hydraulic conductivities in Figures 5 and 6, respectively. Predictions using the Hazen and Sherard expressions tend to over-predict both the field and the laboratory-measured hydraulic conductivities, although these expressions yielded slightly better results for the laboratory hydraulic conductivities. The Hazen correlation was developed for clean sands while the Sherard correlation was developed based on silty soils. Neither provides a good representation for well-graded aggregate with fines. Moulton's expression was the only one specifically developed from correlations with roadway base materials. Results of the Moulton expression better estimated the field measured hydraulic conductivities.

Cedergren (1) has recommended that a drainable base layer on any pavement system be around 1-cm/sec (~ 3000 -ft/day). From the results presented it has been shown that none of the tested materials meet this criterion.

\overline{CU} Tests

Results of the moisture content before and after testing, and effective stress strength parameters from the static \overline{CU} type triaxial compression tests are summarized in Table 3.

Figures 7(a) and (b) present plots of stress difference versus strain and pore pressure versus strain, respectively. Strength tests performed on the material from Lanagan Quarry compacted at optimum water content indicated no cohesion intercept and an angle of internal friction that is representative of a highly dense granular soil (42 degrees). The stress difference-strain relationship was non-linear and continuously increasing until about 15 percent strain after which it leveled out. The pore pressures generated during shearing are representative of dense granular soils and helps to explain this behavior. Positive changes in pore pressures was minimum and

was observed at the beginning of the test up to about 1 percent axial strain, followed by negative changes that steadily continued until about 15 percent to 20 percent strain when they leveled out.

Cyclic, Stress-Controlled Tests

The stress difference-strain response to cyclic loading under stress-controlled conditions was similar to the response observed in the static CU triaxial tests. Negative changes in pore pressures, as high as 140-kPa, occurred almost immediately after beginning the tests and remained negative throughout the test, even during unloading. Figure 8(a) shows the shape and slope of the stress difference-strain curve of a sample tested at an initial effective confining stress of 14-kPa. It is clearly observed that the shape of the curve remained practically unchanged cycle after cycle throughout the test until reaching 20 percent strain. This is attributed to the significant negative pore pressure phenomenon that restrained the sample from dilating, as shown in Figure 8(b). Although the stress levels applied to the samples were less than the maximum stress difference, however, failure was defined by excessive bulging at 20 percent strain (9). This same behavior was also observed in other cyclic tests under stress-controlled conditions performed at lower stress levels under the same effective confining stress of 14-kPa.

Cyclic, Strain-Controlled Tests

The stress-strain response under strain-controlled conditions showed a totally different behavior compared to the stress-controlled type of test. Contrary to the stress-controlled tests, bulging of the samples was not experienced at such low strains; sample appearance remained practically unchanged upon completion of the tests. Figure 9 shows the results of the strain-controlled cyclic triaxial test performed at an effective confining stress of 28-kPa. Samples sheared to strains ranging between 1 percent and 4 percent, and tested at effective confining stresses of 14-kPa and 28-kPa experienced a small drop in pore pressure during the first load cycle, after which changes in pore pressure became positive until the end of the test. Figure 9(a) shows that pore pressures increased rapidly in the first two loading cycles until approaching the total confining pressure of 393 kPa from the third cycle on, and reducing the effective stress in the sample to near zero. Consequently, strength degradation caused a flattening of the stress difference-strain curve slope, which progressed with every load cycle. As seen in Figure 9(a), after applying twenty load cycles the principal stress difference attained was only about 10 percent of the initial maximum principal stress difference in the first cycle and the stress difference-strain curve had flattened out.

PRACTICAL IMPLICATIONS

One of the best ways to prevent damages to roads is to allow for complete and rapid drainage of any water that infiltrates into the pavement system. The specifications for the base materials used in roads should provide for the use of more permeable materials, or provide for alternate means to provide sufficient drainage, e.g. geocomposites. Strength and hydraulic conductivity testing should be performed on these new materials or systems to determine if they are capable of removing all the water that might infiltrate the pavement system in a timely manner, and if it will be strong enough to support the loads imparted by the pavement layers and traffic.

Although this paper is focused on the worst-case scenario of a non- draining base, additional work is being performed to evaluate the performance of freely draining granular bases under drained, partly drained, and cyclic loading conditions to compare the behaviors.

CONCLUSIONS

Using a poorly draining aggregate with low hydraulic conductivity as base material that may become saturated in the long term, compromises the performance and strength of road bases when subjected to cyclic loads. Results of cyclic triaxial tests under saturated, undrained conditions performed on compacted, Type-5 base material indicate that the loading nature has a significant impact on the pore pressure generation, and therefore on the strength of the soil. The strength of samples tested under stress-controlled cyclic loading remained unchanged due to the high negative changes in pore pressures in the sample during loading and locked-in during unloading. On the contrary, the strength of samples tested under strain-controlled cyclic loading to no more than 4 percent strain experienced significant degradation and reduction of effective stress to zero after the second load cycle due to build-up of positive pore pressures. Reductions of as much as 90 percent in principal stress difference were attained after 20 cycles. It is concluded that the current base material has too low of a hydraulic conductivity and may saturate and act in undrained behavior during the cyclic loading of traffic. Under cyclic loading conditions the saturated base loses most of its strength within a few load cycles. This behavior could explain the premature deterioration of some pavements.

ACKNOWLEDGMENTS

The authors wish to acknowledge Dr. John Bowders and Dr. J. Erick Loehr for their immeasurable guidance, assistance, and support during this project. They would also like to acknowledge the valuable assistance of Joseph Chen, Nicolas Pino, Deepak Neupane, and Jeannie Sims (University of Missouri-Columbia Civil and Environmental Engineering students), and Stowe Johnson and Mike Blackwell of MoDOT. The Project Technical Officer is John Donahue (MoDOT). Funding was provided by the Research Development and Technology Unit of the Missouri Department of Transportation, Ray Purvis, Director.

REFERENCES

- 1 Cedergren, H. *Drainage of Highway and Airfield Pavement*. John Wiley and Sons, Inc., New York, 1974.
- 2 Cedergren, H. America's Pavements: World's Largest Bathtubs. *Civil Engineering*, Vol. 64, September 1994, pp. 56-58.
- 3 Moulton, L. *Highway Subdrainage Manual*, Report TS-80-224. FHWA, U.S. Department of Transportation, 1980.
- 4 Cedergren, H. *Seepage, Drainage and Flow Nets*. John Wiley and Sons, Inc., New York, 1989.
- 5 Missouri Department of Transportation. *Materials Specifications*, Section 1007, 1996.
- 6 American Society for Testing Materials, D 698-00. *Standard Test Methods for Laboratory Compaction Characteristics of Soil Using Standard Effort (12,400 ft-lbf/ft³ (600 kN/m³))*, Sect. 4, Vol. 4.08, 2000.
- 7 American Society for Testing Materials, D 5084. *Standard Test Methods for Measurement of Hydraulic Conductivity of Saturated Porous Materials Using a Flexible Wall Permeameter*, Sect. 4, Vol. 4.09, 2000.
- 8 American Society for Testing Materials, D 3385-94. *Standard Test Method for Infiltration Rate of Soils Using Double-Ring Infiltrometer*, Sect. 4 Vol. 4.08, 1994.
- 9 Lee, K., Seed B., *Cyclic Stress Conditions Causing Liquefaction of Sand*, Journal of the Soil Mechanics and Foundations Division, Proceedings of the American Society of Civil Engineers, SM1, January, 1967, p.47-68.

LIST OF TABLES

Table 1 Material Properties, Type 5 Base and Alternate Rock Fill

Table 2 Predicted, Laboratory-Measured and Field-Measured Hydraulic Conductivities of Base Courses

Table 3 Triaxial Test Results for the Lanagan Quarry Sample Based on Maximum Stress Difference Criterion

LIST OF FIGURES

Figure 1 Typical pavement cross-section showing drainage system and possible sources of water.

Figure 2 Constant head permeability (CHP) apparatus.

Figure 3 Cross section view of double ring infiltrometer (DRI) used for in-situ hydraulic conductivity testing of base course.

Figure 4 Laboratory and field hydraulic conductivities, Type 5 base material and alternate rock fill from various field locations in Missouri.

Figure 5 Field hydraulic conductivity and predicted hydraulic conductivity (dry sieve) for all sites tested

Figure 6 Laboratory hydraulic conductivity and predicted hydraulic conductivity (dry sieve) for all sites tested

Figure 7 Results of CU-bar triaxial tests on Lanagan samples (a) Stress difference versus strain at different effective confining stresses. (b) Pore pressures versus strain at different effective stresses.

Figure 8 Stress-controlled cyclic triaxial tests at initial effective confining stress = 14-kPa, (a) Stress difference versus strain, (b) Pore pressure versus strain.

Figure 9 Strain-controlled cyclic test results at initial effective confining stress = 28-kPa, (a) Pore pressure versus strain, (b) Stress difference versus strain.

TABLE 1 Material Properties, Type 5 Base and Alternate Rock Fill

Source	D ₆₀ (mm)	D ₃₀ (mm)	D ₁₅ (mm)	D ₁₀ (mm)	C _u	C _z	% Pass #200 Dry Sieve	% Pass #200 Wet Sieve	g _{dmax} (KN/m ³)	OMC (%)	e	n
Ash Grove Quarry	5.8	1.1	0.3	0.2	38.7	1.4	6	12	21.5	7.0	0.21	0.17
Ash Grove Field	5.5	1.6	0.5	0.2	27.5	2.3	5	17	21.5	7.0	0.21	0.17
Idecker Quarry	9.5	3.7	1.2	0.5	19.0	2.9	3.3	13	19.7	10.0	0.32	0.24
Idecker Field	5.9	1.4	0.4	0.2	28.1	1.6	5	18	19.7	10.0	0.32	0.24
Lanagan Quarry	4.0	1.0	0.5	0.4	11.4	0.7	3	13	22.2	6.0	0.17	0.15
Riggs Quarry	7.0	1.3	0.2	0.1	50.0	1.7	6	19	21.5	8.0	0.21	0.17
Crawford Co.	7.0	1.7	0.5	0.3	23.3	1.4	1.7	14	21.8	8.0	0.19	0.16
Taney Co.	4.8	1.1	0.4	0.2	23.8	1.3	5.7	15	21.8	7.7	0.19	0.16

1-in = 25.4-mm
 6.361-lb/ft³ = 1-KN/m³

TABLE 2 Predicted, Laboratory-Measured and Field-Measured Hydraulic Conductivities of Base Courses

Source	? g _a (KN/m ³)	w (%)	Void Ratio	Hazen k (cm/sec)	Predicted k			
					Sherard k (cm/sec)	Moulton k (cm/sec)	Lab k (cm/sec)	Field k (cm/sec)
Ash Grove Quarry	20.6	8	0.21	2.25x10 ⁻²	2.94x10 ⁻²	4.1x10 ⁻⁵	2.8x10 ⁻³	1.9x10 ⁻³
Ash Grove Field	21.2	8	0.21	4.0x10 ⁻²	7.09x10 ⁻²	7.01x10 ⁻⁵	3.0x10⁻⁶	1.9x10 ⁻³
Idecker Quarry	18.8	9	0.32	2.5x10 ⁻¹	5.04x10 ⁻¹	3.24x10 ⁻³	8.8x10 ⁻²	4.6x10 ⁻⁵
Idecker Field	21.8	9	0.32	4.41x10 ⁻²	5.60x10 ⁻²	7.02x10 ⁻⁴	3.0x10⁻⁷	4.60x10 ⁻⁵
Lanagan Quarry	21	4	0.17	1.23x10 ⁻¹	8.75x10 ⁻²	7.05x10 ⁻⁵	5.4x10 ⁻³	9.7x10 ⁻⁵
Riggs Quarry	21.7	9	0.21	1.96x10 ⁻²	1.85x10 ⁻²	3.30x10 ⁻⁵	5.20x10 ⁻³	3.70x10 ⁻⁵
Crawford Co.	21.4	8.8	0.19	9.0x10 ⁻²	8.75x10 ⁻²	1.43x10 ⁻⁴	4.5x10⁻⁶	9.10x10 ⁻⁵
Taney Co.	22.7	7.9	0.19	4.00x10 ⁻²	6.32x10 ⁻²	3.64x10 ⁻⁵	3.00x10 ⁻⁴	1.90x10 ⁻⁵

Values in bold represent flexible wall permeameter tests

6.361-lb/ft³ = 1-KN/m³

1-cm/sec = 2835-ft/day

TABLE 3 Triaxial Test Results for the Lanagan Quarry Sample Based on Maximum Stress Difference Criterion

Maximum Dry Unit Weight (kN/m ³)	Optimum Water Content (%)	Sample No.	Effective Consol. Stress (kPa)	w (%) molding	w (%) during shear	Peak Eff. Principal Stress Difference (kPa)	Peak Volumetric Strain (%)	Effective Friction Angle	Effective Cohesion
22.2	6	1	13.8	6	8.9	97.4	16.2	42	0
		2	27.6	6.5	8.7	115	20.4		
		3	41.4	6	9	116.6	12.7		

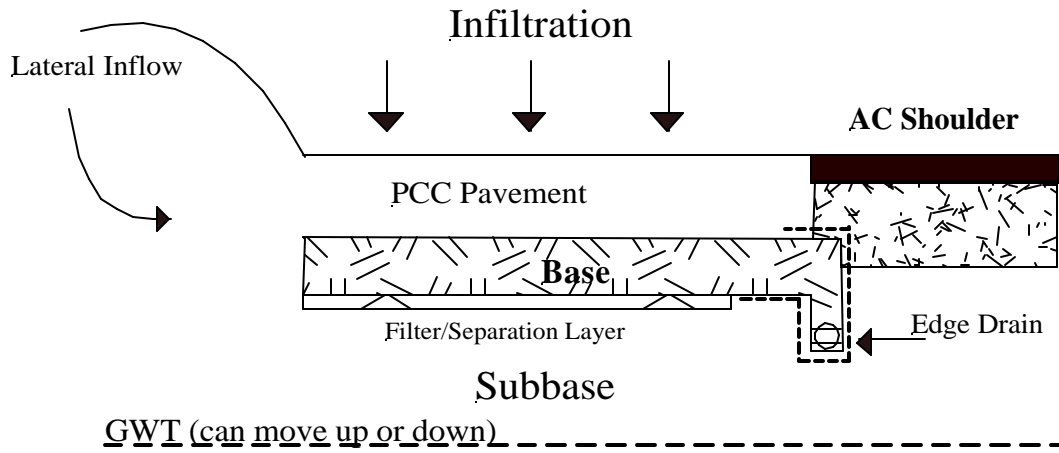


Figure 1 Typical pavement cross-section showing drainage system and possible sources of water.

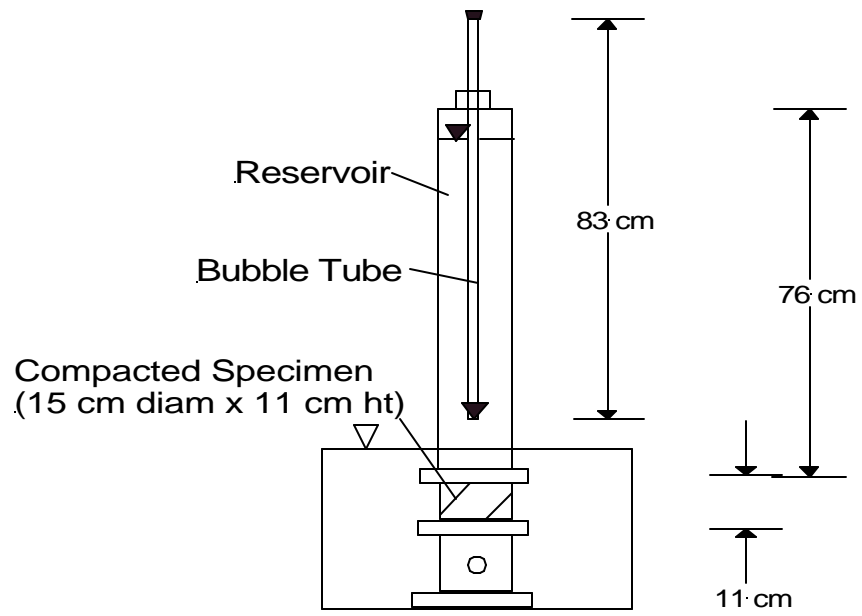


FIGURE 2 Constant head permeability (CHP) apparatus

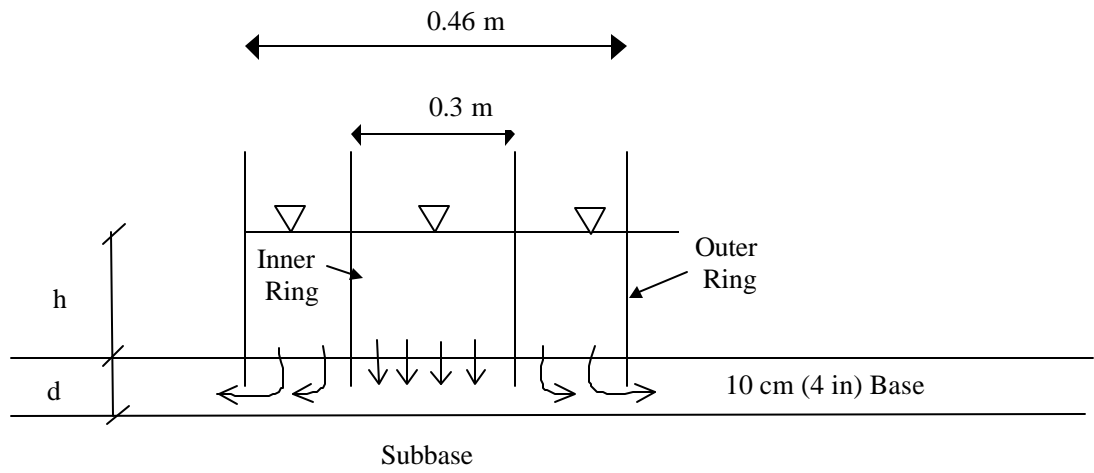


FIGURE 3 Cross section view of double ring infiltrometer (DRI) used for in-situ hydraulic conductivity testing of base course.

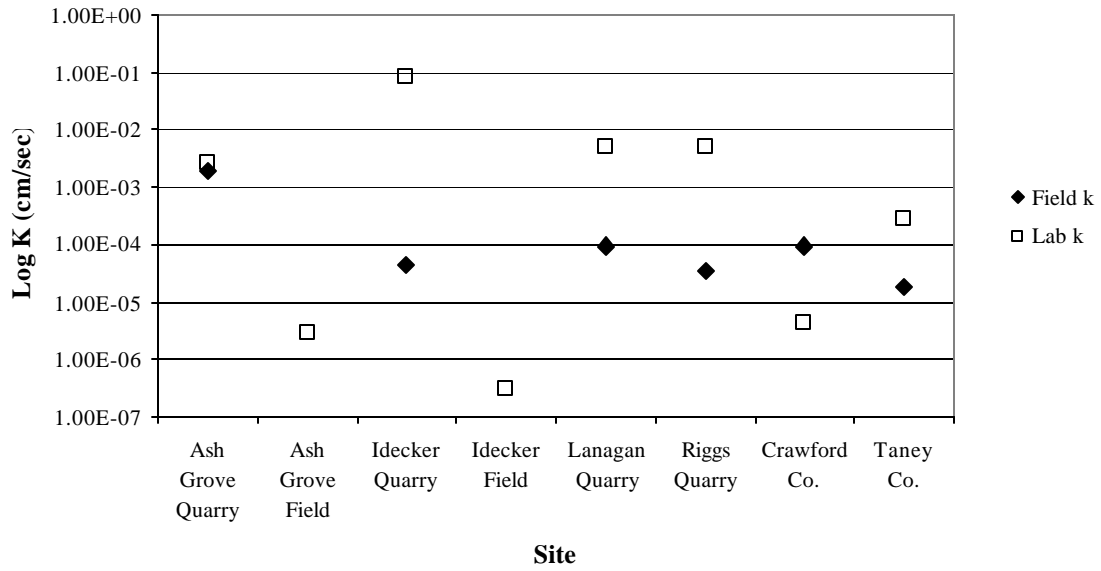


FIGURE 4 Laboratory and field hydraulic conductivities, Type 5 base material and alternate rock fill from various field locations in Missouri.

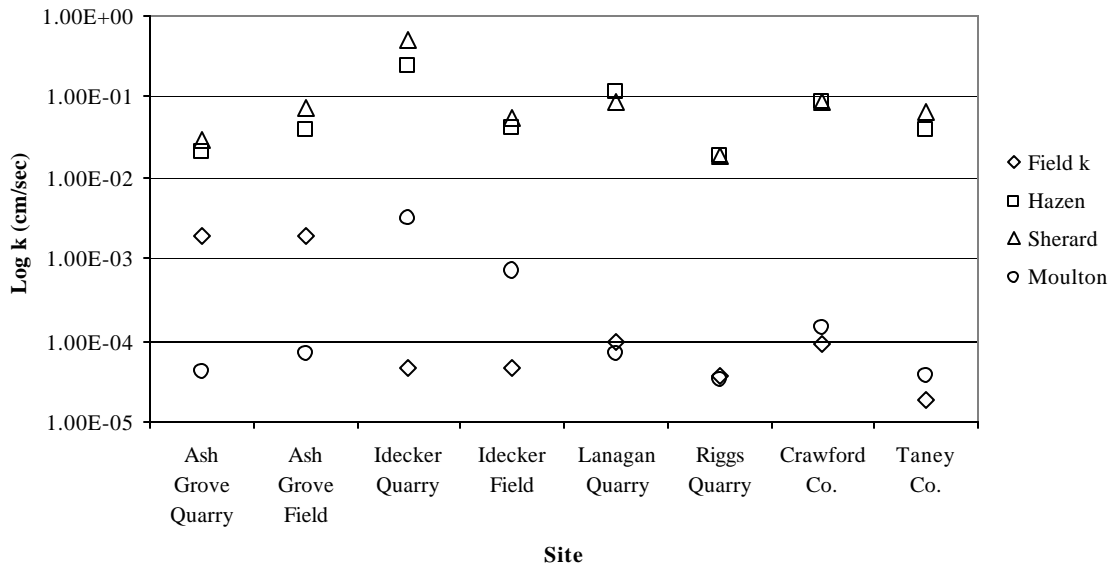


FIGURE 5 Field hydraulic conductivity and predicted hydraulic conductivity (dry sieve) for all sites tested

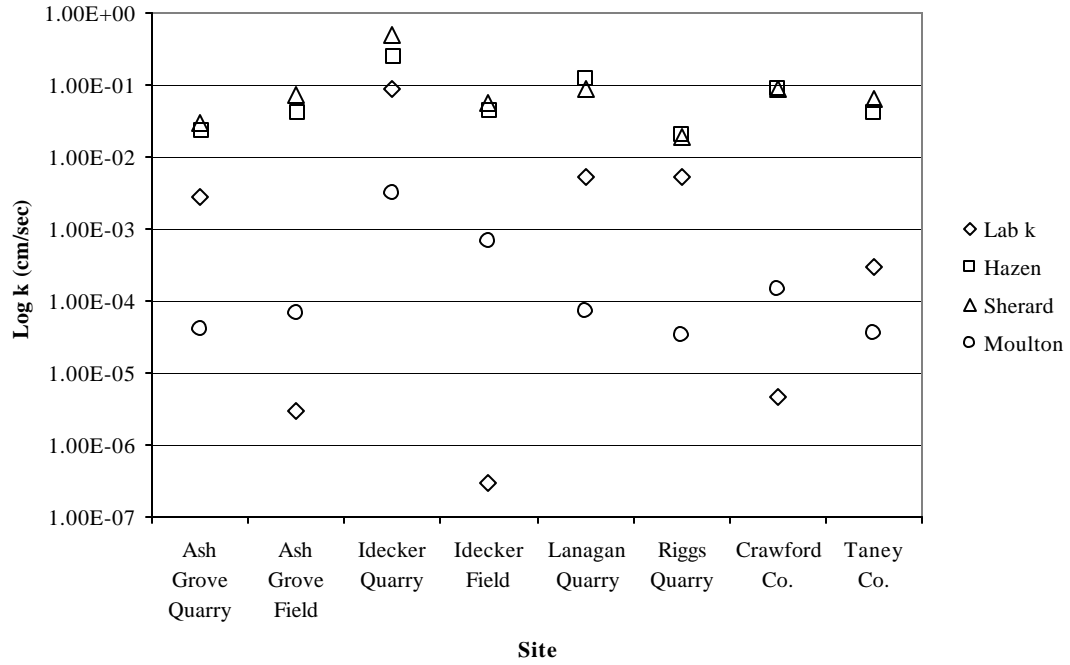


FIGURE 6 Laboratory hydraulic conductivity and predicted hydraulic conductivity (dry sieve) for all sites tested

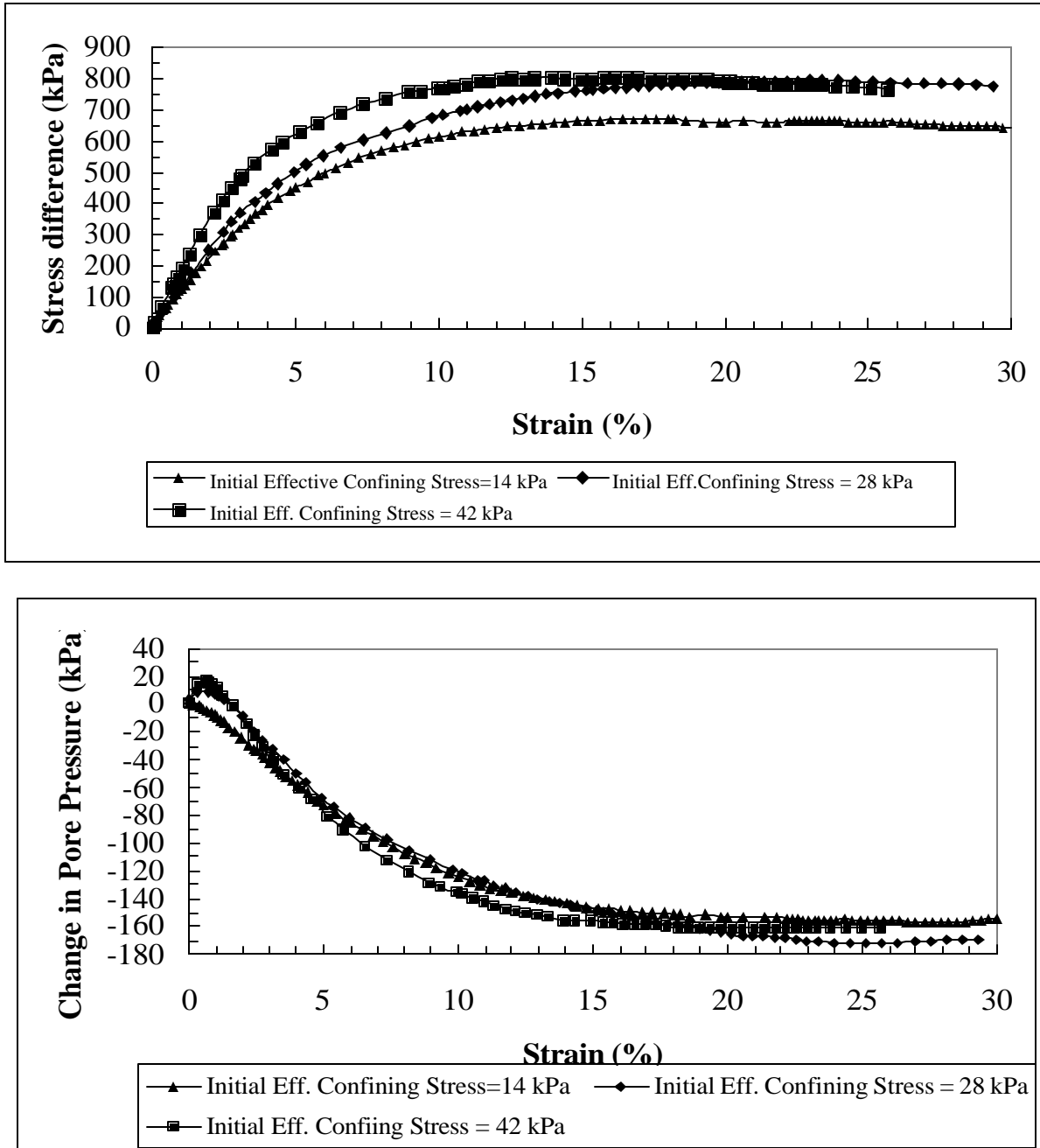


FIGURE 7 Results of CU-bar triaxial tests on Lanagan samples (a) Stress difference versus strain at different effective confining stresses. (b) Change in pore pressures versus strain at different effective stresses

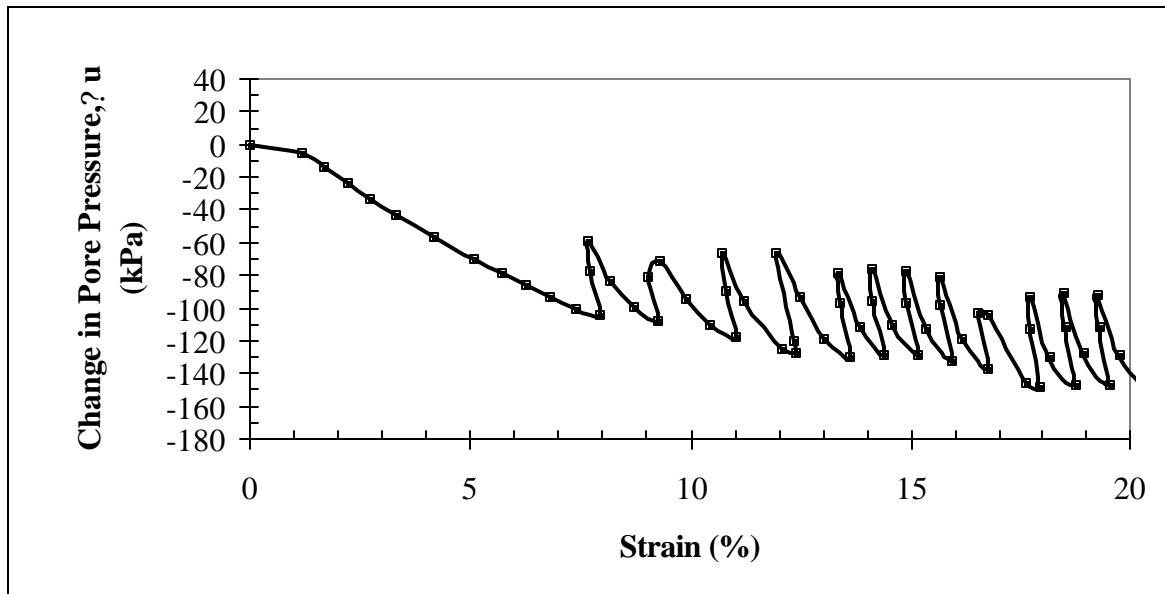
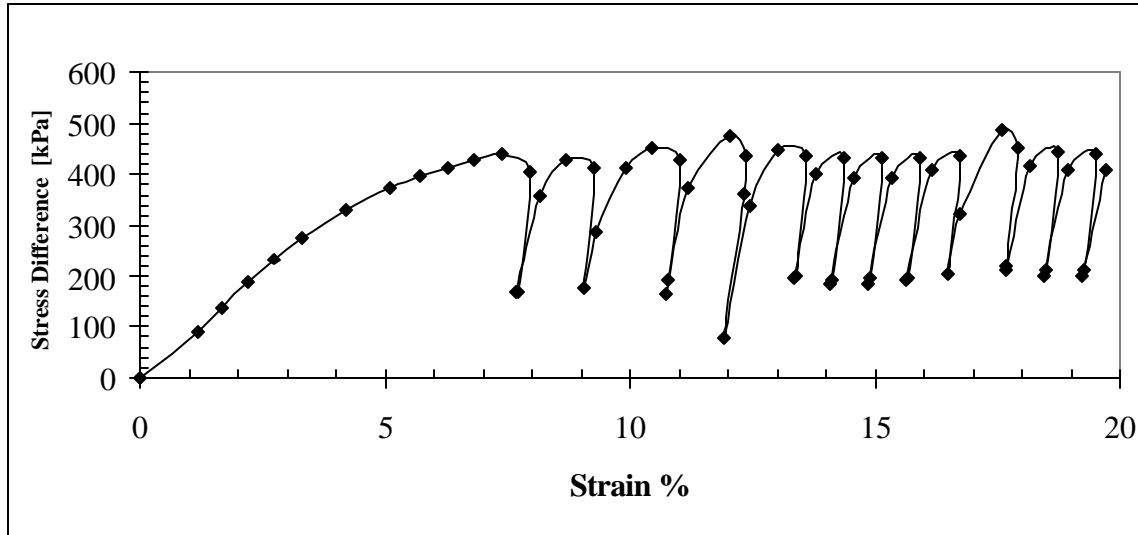


FIGURE 8 Stress-Controlled cyclic triaxial tests at initial effective confining stress =14-kPa, (a) Stress difference versus strain, (b) Change in pore pressure versus strain

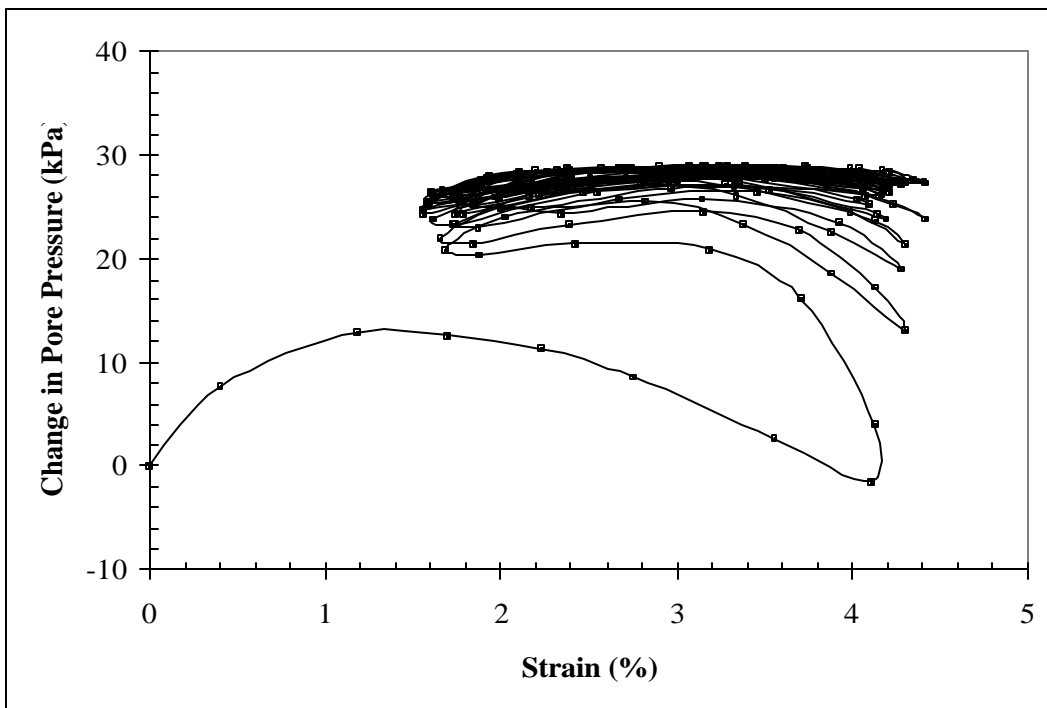
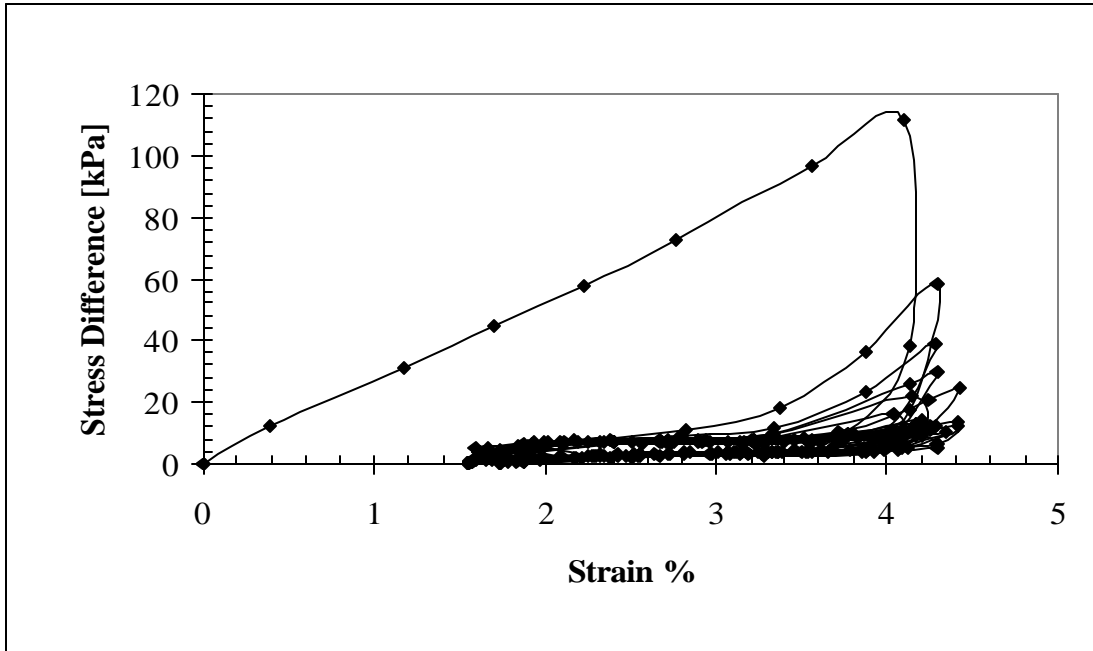


FIGURE 9 Strain-controlled cyclic triaxial test results at initial effective confining stress= 28-kPa, (a) Stress difference versus Strain, (b) Change in pore pressure versus strain.